J Inorg Organomet Polym (2015) 25:780–786
DOI 10.1007/s10904-014-0159-0

Facile Fabrication and Characterization of Three-Dimensional Ordered Films of TiO_2 Hollow-Spheres

Yang Chen · Zhaofang Tang · Zhigang Chen

Received: 20 November 2014 / Accepted: 26 December 2014 / Published online: 31 December 2014

Abstract High-quality three-dimensional ordered TiO_2 hollow-spheres (3DOH-TiO_2) materials were fabricated using polystyrene spheres colloidal crystals (ca. 290 nm in center-to-center distance) as sacrificial templates and titanium tetrachloride as titanium sources. The obtained samples were characterized by X-ray diffraction, Raman spectroscopy, field emission scanning electron microscopy (FESEM), high resolution transmission electron microscopy (HRTEM) and N_2 adsorption–desorption. The results showed that the films are composed of a closely packed, hexagonal array of the TiO_2 hollow-spheres with a center–center separation of ca. 260 nm. The homogeneity in the shell thickness (ca. 40 nm), the physical contact among adjacent hollow-spheres, and the long-range order in the sample were also confirmed by FESEM and TEM analysis. HRTEM results indicated the walls of the hollow-spheres consist of anatase TiO_2 nanoparticles (15–20 nm). The porous framework structure of the 3DOH-TiO_2 films was further characterized using N_2 physical adsorption, and the Brunauer–Emmett–Teller specific surface area and the total pore volume are around 77.72 m^2/g and 0.262 cm^3/g, respectively.

Y. Chen (✉) · Z. Tang
School of Materials Science and Engineering, Changzhou University, Changzhou 213164, Jiangsu, China
e-mail: cy.jpu@126.com

Y. Chen · Z. Chen
Jiangsu Key Laboratory for Environment Functional Materials, Suzhou University of Science and Technology, Suzhou 215009, Jiangsu, China

Z. Chen
Department of Chemistry and Bioengineering, Suzhou University of Science and Technology, Suzhou 215009, Jiangsu, China

Keywords Polystyrene microsphere · Colloidal crystal template · Titania · Hollow sphere · 3D ordered structure

1 Introduction

Colloidal crystals [1] are three-dimensional (3D) periodic structures fabricated through the ordered packing of monodisperse microspheres (silica, polystyrene or polymethylmethacrylate). The self-assembly of 3D ordered colloidal crystals based on monodispersed particles has been intensively studied, and many methods [2–6] have been reported to assemble monodispersed colloids into ordered colloidal crystals, such as gravity sedimentation, centrifugation, electrophoretic deposition, filtration and spin-coating.

Ordered porous materials [7, 8] with periodical nanostructure, tunable pore size, large entrance and easily functionalizable surface, have recently attracted great attention for their possible potential applications in photonic crystals, separation, catalysis, drug delivery and electrochemical cells. Many methods have been developed to fabricate ordered porous materials, including soft lithograph, emulsion templating synthesis and so on. The most conventional approach is the hard-templating process with colloidal crystals as the sacrificial templates.

In the past decades, 3D ordered macro-porous (3DOM) materials with various compositions have been extensively studied, including 3DOM-C [9], -TiO_2 [10], -SnO_2 [11], -Fe_2O_3 [12], -Y_2O_3 [12], -SiO_2 [13], -$Li_4Ti_5O_{12}$ [14] and so on. However, there are few reports on the fabrication of 3D ordered hollow-spheres (3DOH) films using colloidal crystals templates. For example, Zhong et al. [15] prepared 3DOH-SnO_2 materials by templating their sol–gel precursor solutions against crystalline arrays of monodisperse PS

beads. Besides, Li et al. [16] fabricated 3D-ordered films of TiO_2 hollow spheres (20–30 nm in shell thickness) by using 3D-ordered latex films as a templates and titanium(IV) butoxide as titanium source. The photonic stop band was observed for the 3DOH-TiO_2 film, which could be tunable by the inner core size and the shell thickness. Recently, Dinh et al. [17] reported the construction of 3D assembly of thin-shell Au/TiO_2 hollow spheres via silica colloidal crystals as templates and titanium butoxide as starting materials. And the results showed that the designed 3DOH-Au/TiO_2 exhibited a high surface area, photonic behavior, and enhanced light scattering effects. However, the long-range order in the hollow-spheres films needs to be improved.

In order to obtain highly ordered 3DOH-TiO_2 films, we reported a simple, efficient and cost-effective route using high-quality polystyrene (PS) colloidal crystals as templates and titanium tetrachloride as titanium sources. The as-synthesized 3DOH-TiO_2 materials exhibited a highly 3D ordered structure with a large surface area, and the hollow-spheres were orderly arranged through hexangular and square arrays. And the TiO_2 hollow-spheres were connected to their neighbors through pores.

2 Experimental

2.1 Chemicals

Styrene (St), potassium persulfate (KPS), methylacrylic acid (AA), concentrated sulphuric acid (98 wt%, H_2SO_4), hydrogen peroxide (30 wt%, H_2O_2), titanium tetrachloride ($TiCl_4$), acetone, and ethanol were purchased in their reagent grades from Shanghai Chemical Reagent Co. (China), and used without further purification. Deionized (DI) water was used for all experiments.

2.2 Fabrication of PS Colloids and Colloidal Crystal Templates

Monodisperse PS colloids were prepared via a soap-free emulsion polymerization process according to previous report [18]. In a typical synthesis, 50 g of DI water, 5 g of St and 0.75 g of AA were added into a three-necked bottle equipped with a magnetic stirrer, a thermometer with a temperature controller and a N_2 inlet. This mixture was deoxygenated by bubbling N_2 under magnetic stirring at room temperature for 30 min and then placed into an oil bath at 70 °C, followed by addition of initiator (0.13 g of KPS dissolved in 50 g of DI water, the pH of the solution was adjusted to 8 by ammonia) to initiate the polymerization. The polymerization reaction was performed in constant N_2 protection and magnetic stirring for 7 h. Finally, the latex dispersion was purified and concentrated by a centrifugation procedure.

The glass slips (3 cm × 2 cm × 0.1 cm) used as substrates were firstly ultrasonic cleaned in acetone, ethanol and DI water, and then immersed in piranha solution (H_2O_2/H_2SO_4, 3/7, v/v) for 10 min under 80 °C to obtain hydrophilic surfaces. The multi-layer PS colloidal crystals were assembled by a modified horizontal deposition method [19]. Briefly, PS colloidal suspension (ca. 5 wt%) was dropped on the substrate to spread on the whole surface under ambient conditions for self-assembly and drying at 30 °C and a relative humidity of 60 %. Before infiltration with the TiO_2 precursor solution, the templates were dried at 105 °C for 10 min to enhance their structure stability.

2.3 Preparation of 3DOH-TiO_2 Films

According to the method described in literature [20], the aqueous $TiCl_4$ (titanium precursor) solutions were prepared by slowly adding, drop-wise, a given amount of DI water into a certain amount of $TiCl_4$. When water contacts with $TiCl_4$ excess heat explosively generating from the exothermic reaction was removed by constantly shaking in ice-water bath. The concentration of colorless aqueous $TiCl_4$ solution was adjusted to about 0.2 M. And the aqueous $TiCl_4$ solutions were kept in ice-water bath. Subsequently, the pretreated templates were immersed vertically into the aqueous $TiCl_4$ solution for 12 h. During the immersion process, the surfaces of the PS spheres could be covered with TiO_2 precursor by capillary force. Then, the substrates were drawn out and the template/TiO_2-precursor composites were dried for 24 h in air. These procedures were performed in a fume hood. Finally, the as-prepared composites were heated in an oven to 500 °C at 2 °C/min, held for 2 h to remove the templates and cooled slowly to room temperature.

2.4 Characterization

The morphology observation was performed by a JSM-6360LA scanning electron microscope (SEM, JEOL, Japan) and an S-4800 field emission SEM (FESEM, Hitachi, Japan) at an accelerating rate of 15 kV. High resolution transmission electron microscopy (HRTEM) analyses were carried out by a JEM-2100 electron microscope (JEOL, Japan) with an accelerating voltage of 200 kV to observe the ordered hollow structure of the films. X-ray diffraction (XRD) pattern was measured on a D/max 2500 X-ray diffractometer (Rigaku, Japan) with Cu Kα radiation to determine the phase structure of the as-prepared samples. Raman spectrum analysis was conducted using a Renishaw inVia spectrometer. Nitrogen adsorption–desorption

isotherm was obtained by an ASAP2020 (Micromeritics Instruments, USA) nitrogen adsorption apparatus. The surface area and the pore size distribution were calculated by the Brunauer–Emmett–Teller (BET) and the Barret–Joyner–Halender (BJH) methods, respectively.

3 Results and Discussion

Figure 1 exhibits the SEM images of the PS spheres-based colloidal crystal. The high-magnification top view (Fig. 1a) indicated that the PS colloids have a uniform center-to-center distance of ca. 290 nm, and the obtained templates possess typical face-centered cubic packing structure with (111) plane parallel to the substrate. From the low-magnification SEM image (inset in Fig. 1a), individual defects such as vacancies and voids can also be observed. The cross-sectional view (Fig. 1b) revealed that the multi-layer colloidal crystal displays a 3D ordered structure with close-packed arrangement.

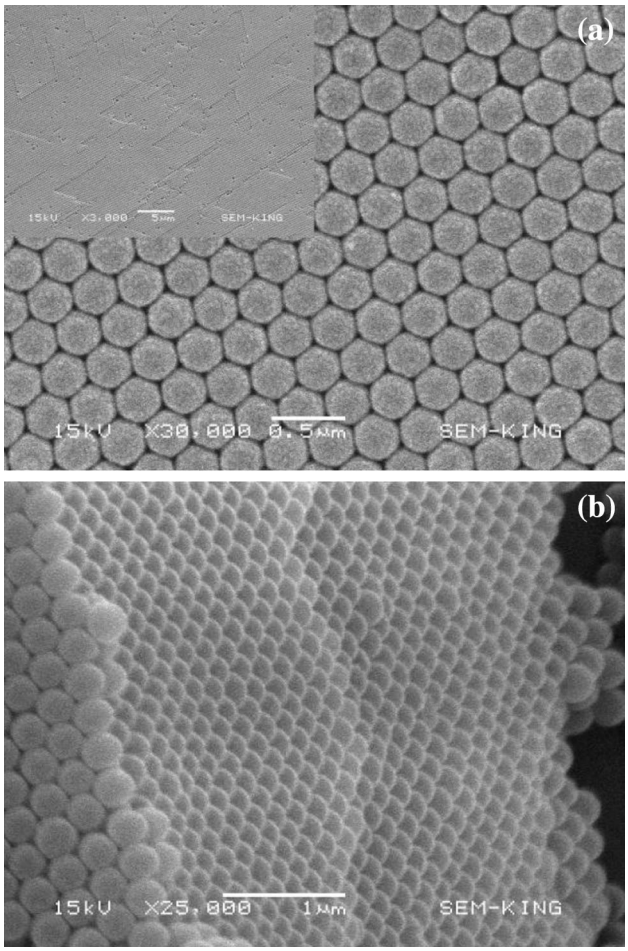

Fig. 1 SEM images of colloidal crystal templates: **a** top view, **b** cross-sectional view

The XRD pattern of the 3DOH-TiO_2 samples is presented in Fig. 2. The obtained diffraction peaks were matched well with the JCPDS Card (21-1272) indicating the body-centered tetragonal anatase phase of TiO_2. The sharp diffraction peaks at $2\theta = 25.3°$ (101), 37.8° (004), 47.9° (200), 53.9° (105), 62.7° (204), 68.8° (116) and 75.1° (215) were corresponds to the lattice plane of anatase phase. The absence of the diffraction peaks at $2\theta = 27.5°$ (110) and 30.8° (121) corresponds to rutile [21] and brookite [22] phase confirms that the as-synthesized samples is pure anatase phase. The crystallite sizes were calculated from the broadening of the anatase (101) peak according to the Scherer's formula ($D = k\lambda/\beta\cos\theta$), where D is the crystallite size (nm), k is the shape constant (0.9), λ is the wave length of Cu Kα radiation (1.5406 Å), θ is the diffraction angle (°) and β is the full width at half

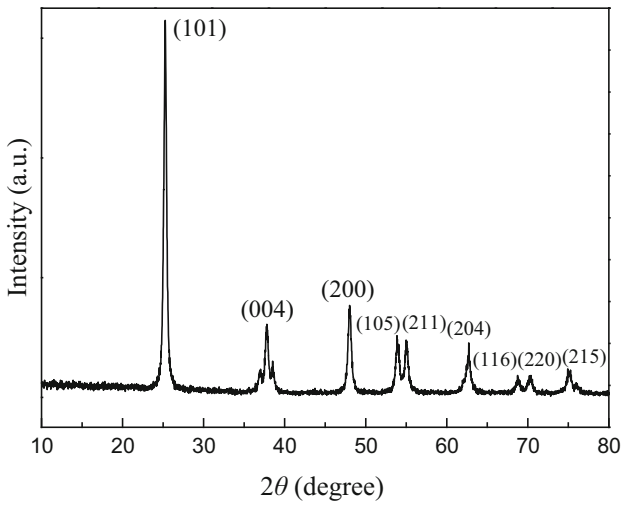

Fig. 2 XRD pattern of 3DOH-TiO_2 samples

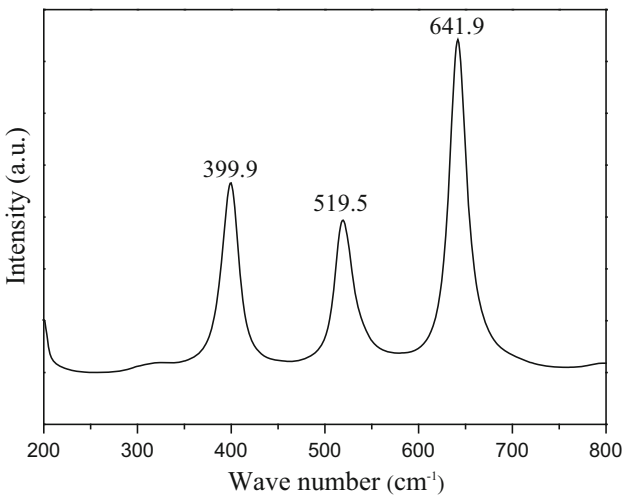

Fig. 3 Raman spectrum of 3DOH-TiO_2 samples

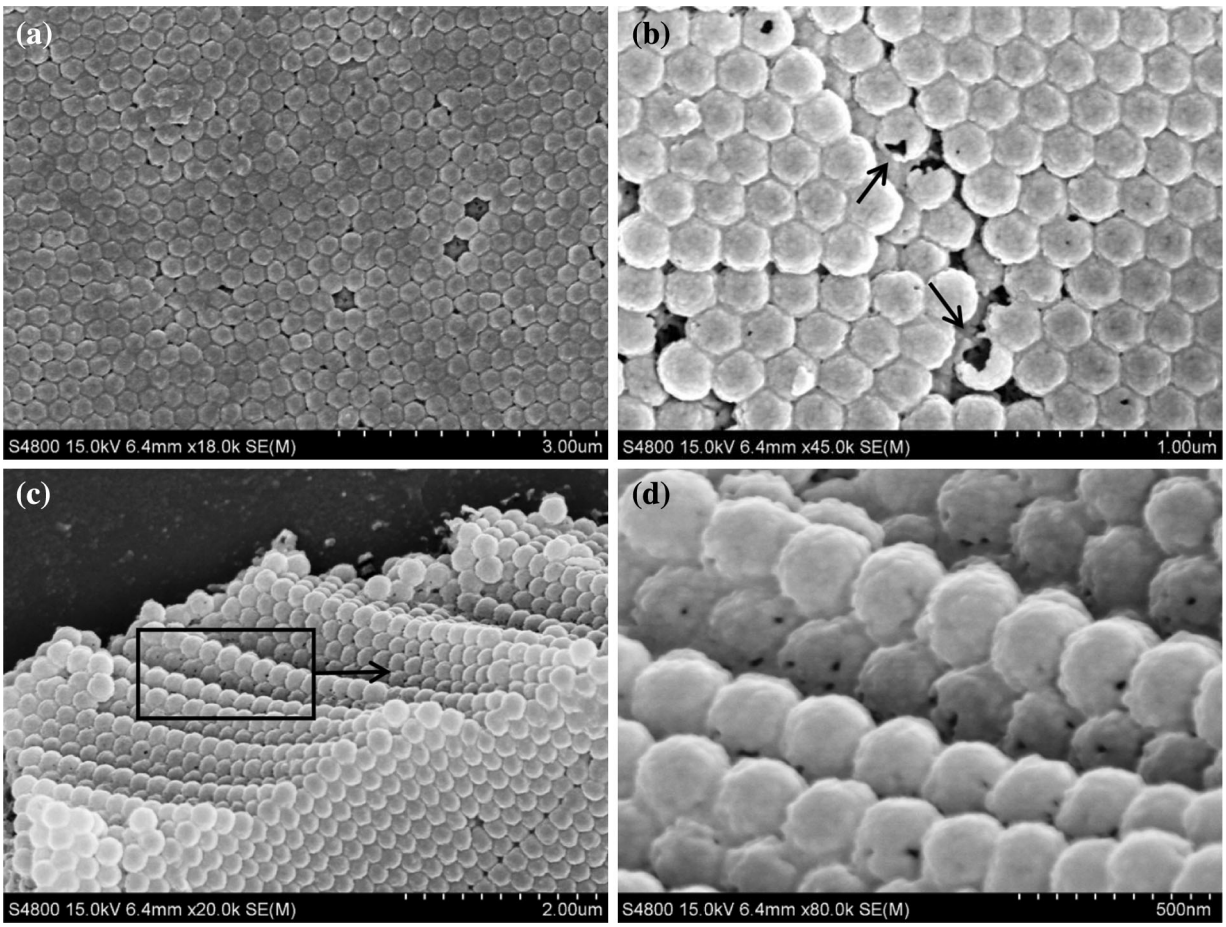

Fig. 4 FESEM images of 3DOH-TiO_2 samples: **a**, **b** top view, **c**, **d** cross-sectional view

maximum. The crystallite size of the calcined anatase TiO_2 was found to be ca. 23 nm.

Figure 3 shows the Raman spectrum of the 3DOH-TiO_2 samples. The bands at ca. 399.9, 519.5 and 641.9 cm^{-1} corresponds to the characteristic bands [23] of crystalline anatase TiO_2. Furthermore, the absence of bands at ca. 445 and 612 cm^{-1} indicates the absence of rutile phase TiO_2 [24]. The Raman and XRD results also confirmed that the obtained samples are complete anatase phase without any phase impurities.

By comparison with the bare colloidal crystal template (Fig. 1), the surface of the 3DOH-TiO_2 samples became rougher (Fig. 4), thus indicating the formation of TiO_2 hollow-spheres. From the top-view FESEM images (Fig. 4a), it can be observed that the film is composed of a closely packed, hexagonal array of TiO_2 spheres, indicating that the 3D ordered assembly structure of template was retained after removal of the PS cores to obtain hollow-spheres. The high-magnification FESEM image (Fig. 4b) shows some broken particles which clearly indicate the hollow structure of the TiO_2 spheres. Furthermore, the hollow spheres are connected to their neighbors through pores. The center–center separation between two neighboring hollow-spheres estimated from the FESEM was about 260 nm, around 10.3 % of shrinkage of the lattice structure compared to the PS templating spheres. The cross-section FESEM image (Fig. 4c) exhibits the TiO_2 hollow-spheres closely packed along the direction perpendicular to the surface. As shown in Fig. 4d, the presence of holes on the shell can also be observed, and these holes might be formed during the removal of the PS cores in calcination process. The homogeneity in shell thickness (ca. 40 nm), the physical contact among adjacent hollow spheres, and the long-range order in the sample are clearly seen in these FESEM images.

The shape, structure and wall thickness of the 3DOH-TiO_2 samples was further characterized by HRTEM (Fig. 5). The low-magnification TEM image (Fig. 5a) revealed that the sample is an assembly of uniform TiO_2 hollow-spheres. Moreover, well-defined hollow-spheres can be observed from the edge image of the sample (Fig. 5b). As confirmed by high-magnification TEM image (Fig. 5c), the obtained TiO_2 hollow-spheres are composed of nano-particles with a size of 15–20 nm. The shell

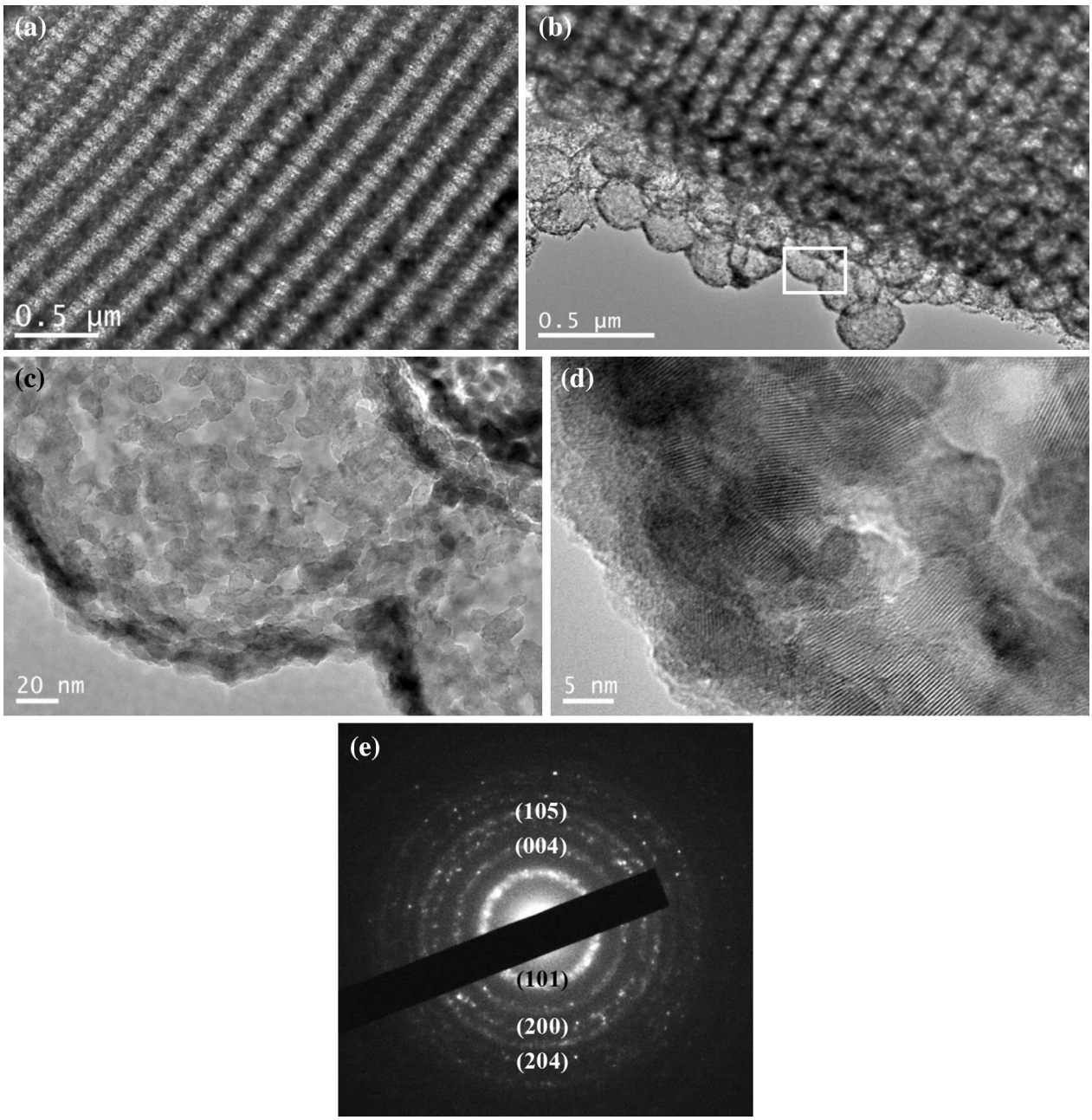

Fig. 5 TEM images (**a**, **b**), HRTEM image (**c**, **d**) and the corresponding SAED pattern (**e**) of 3DOH-TiO_2 samples

thickness of the TiO_2 hollow-spheres is 30–40 nm, which is consistent with the value estimated by FESEM. The high resolution TEM image (Fig. 5d) shows the lattice fringes of TiO_2, indicating the highly crystalline nature of TiO_2 shells. The lattice fringe with a spacing of ca. 0.35 nm can be assigned to the (101) lattice plane of anatase TiO_2. A selected area electron diffraction pattern taken from a single TiO_2 hollow-sphere (Fig. 5e) shows five diffuse diffraction rings, which can be indexed as the (101), (004), (200), (105) and (204) planes of anatase TiO_2, starting from inner to outer ring, respectively. Such a polycrystalline structure ensures the porosity of the films [25], which can further be confirmed by the nitrogen adsorption/desorption measurements.

The porous structure of the 3DOH-TiO_2 samples was characterized using N_2 physical adsorption at 77 K. As shown in Fig. 6, the pore size distribution calculated BJH model on the adsorption branch reveals maxima in the range 3–15 nm, indicating the porous shell of 3DOH-TiO_2 samples. The BET surface area and the total pore volume of the sample are found to be 77.72 m^2/g and 0.262 cm^3/g, respectively. The high BET surface area and large porosity

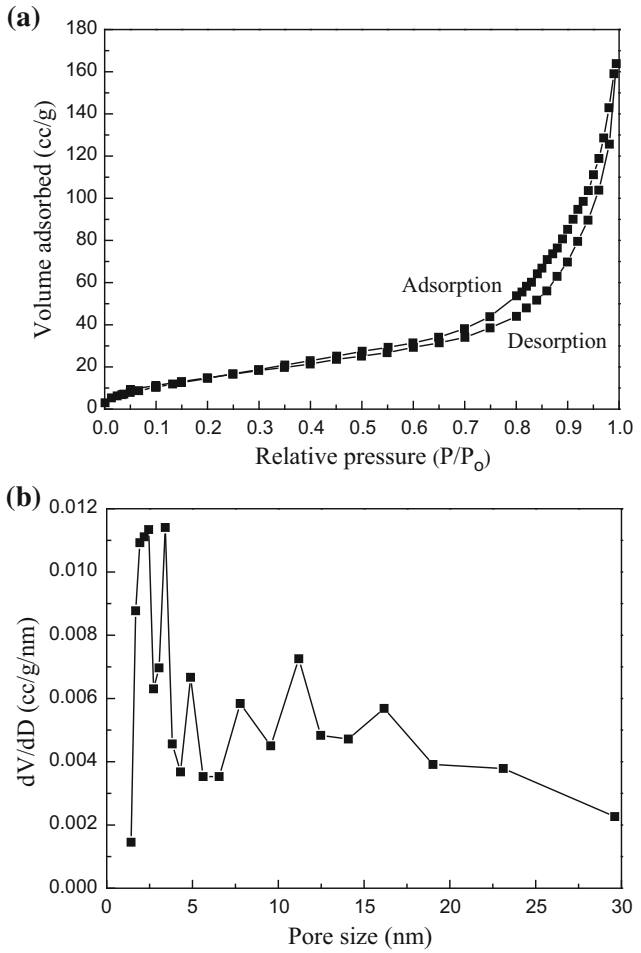

Fig. 6 Nitrogen sorption isotherms (**a**) and pore size distribution (**b**) of 3DOH-TiO_2 samples

illustrate the porous structure of the sample. Therefore, these results demonstrate 3D interconnected TiO_2 hollow-spheres with porous shells.

In summary, the highly ordered TiO_2 hollow-sphere films with a large area have been constructed using a sample experimental setup. The lattice structure of the film is a closely packed face-centric-cubic arrangement. These materials can be considered promising for applications such as photonic crystals, photocatalysts, dye-sensitized solar cells and so forth.

4 Conclusions

Three-dimensional ordered TiO_2 hollow-spheres (3DOH-TiO_2) films were synthesized using PS colloidal crystals as templates via a facile and efficient method. FESEM results revealed that the hollow-spheres are orderly arranged through hexangular and square arrays, and the TiO_2 hollow-spheres are connected to their neighbors through pores. The center–center separation of the 3DOH-TiO_2 is about 260 nm, and the thickness of the hollow shells is ca. 40 nm. HRTEM results confirmed that the porous walls of the hollow-spheres are relatively rough and composed of tiny anatase TiO_2 particles. The size of the TiO_2 nanoparticles is about 15–20 nm, as demonstrated by HRTEM. This approach can be applied in the fabrication of the 3DOH-TiO_2 films with desired void size by selecting the PS colloidal crystal templates with suitable diameter.

Acknowledgments The work was supported financially by the Applied Basic Research Project of Suzhou City (SYG201316) and the Key Laboratory for Environment Functional Materials of Jiangsu Province (SJHG1302).

References

1. A. Stein, B.E. Wilson, S.G. Rudisill, Design and functionality of colloidal-crystal-templated materials-chemical applications of inverse opals. Chem. Soc. Rev. **42**, 2763–2803 (2013)
2. H. Li, F. Marlow, Controlled arrangement of colloidal crystal strips. Chem. Mater. **17**, 3809–3811 (2005)
3. D.D. Brewer, J. Allen, M.R. Miller, J.M. de Santos, S. Kumar, D.J. Norris, M. Tsapatsis, L.E. Scriven, Mechanistic principles of colloidal crystal growth by evaporation-induced convective steering. Langmuir **24**, 13683–13693 (2008)
4. C.I. Aguirre, E. Reguera, A. Stein, Colloidal photonic crystal pigments with low angle dependence. ACS Appl. Mater. Interfaces **2**, 3257–3262 (2010)
5. J. Chen, P. Dong, D. Di, C. Wang, H. Wang, J. Wang, X. Wu, Controllable fabrication of 2D colloidal-crystal films with polystyrene nanospheres of various diameters by spin-coating. Appl. Surf. Sci. **270**, 6–15 (2013)
6. N.F. Bunkin, V.S. Gorelik, V.A. Kozlov, A.V. Shkirin, N.V. Suyazov, Colloidal crystal formation at the "nafion-water" interface. J. Phys. Chem. B **118**, 3372–3377 (2014)
7. J.I.L. Chen, G. Freymann, V. Kitaev, Effect of disorder on the optically amplified photocatalytic efficiency of titania inverse opals. J. Am. Chem. Soc. **129**, 1196–1202 (2007)
8. D.V. Talapin, J. Lee, M.V. Kovalenko, E.V. Shevchenko, Prospects of colloidal nanocrystals for electronic and optoelectronic applications. Chem. Rev. **110**, 389–458 (2010)
9. S.Q. Fan, B.Z. Fang, J.H. Kim, B. Jeong, C. Kim, J.S. Yu, J.J. Ko, Ordered multimodal porous carbon as highly efficient counter electrodes in dye-sensitized and quantum-dot solar cells. Langmuir **26**, 13644–13649 (2010)
10. Z. Cai, J. Teng, Z. Xiong, Y. Li, Q. Li, X. Lu, X.S. Zhao, Fabrication of TiO_2 binary inverse opals without overlayers via the sandwich-vacuum infiltration of precursor. Langmuir **27**, 5157–5164 (2011)
11. S. Xu, F. Sun, F. Gu, Y. Zuo, L. Zhang, C. Fan, S. Yang, W. Li, Photochemistry-based method for the fabrication of SnO_2 monolayer ordered porous films with size-tunable surface pores for direct application in resistive-type gas sensor. ACS Appl. Mater. Interfaces **6**, 1251–1257 (2014)
12. M. Davis, D.A. Ramirez, L.J. Hope-Weeks, Formation of three-dimensional ordered hierarchically porous metal oxides via a hybridized epoxide assisted/colloidal crystal templating approach. ACS Appl. Mater. Interfaces **5**, 7786–7792 (2013)
13. W. Chae, D. Van Gough, S. Ham, D.B. Robinson, P.V. Braun, Effect of ordered intermediate porosity on ion transport in hierarchically nanoporous electrodes. ACS Appl. Mater. Interfaces **4**, 3973–3979 (2012)

14. E.M. Sorensen, S.J. Barry, H. Jung, J.M. Rondinelli, J.T. Vaughey, K.R. Poeppelmeier, Three-dimensionally ordered macroporous $Li_4Ti_5O_{12}$: effect of wall structure on electrochemical properties. Chem. Mater. **18**, 482–489 (2006)
15. Z. Zhong, Y. Yin, B. Gates, Y. Xia, Preparation of mesoscale hollow spheres of TiO_2 and SnO_2 by templating against crystalline arrays of polystyrene beads. Adv. Mater. **12**, 206–209 (2000)
16. Y. Li, T. Kunitake, S. Fujikawa, Efficient fabrication and enhanced photocatalytic activities of 3D-ordered films of titania hollow spheres. J. Phys. Chem. B **110**, 13000–13004 (2006)
17. C. Dinh, H. Yen, F. Kleitz, T. Do, Three-dimensional ordered assembly of thin-shell Au/TiO_2 hollow nanospheres for enhanced visible-light-driven photocatalysis. Angew. Chem. Int. Ed. **53**, 6618–6623 (2014)
18. Y. Chen, R.W. Long, Z.G. Chen, Polishing behavior of PS/CeO_2 hybrid microspheres with controlled shell thickness on silicon dioxide CMP. Appl. Surf. Sci. **257**, 8679 (2011)
19. Z. Cai, J. Teng, Q. Yan, X.S. Zhao, Solvent effect on the self-assembly of colloidal microspheres via a horizontal deposition method. Colloids Surf. A **402**, 37–44 (2012)
20. L. Ma, J. Ji, F. Yu, N. Ai, H. Jiang, Post-synthesis of TiO_2/MCM-41 from aqueous $TiCl_4$ solution: structure characteristics and epoxy catalytic activity. Microporous Mesoporous Mater. **165**, 6–13 (2013)
21. G. Chen, J. Chen, Z. Song, C. Srinivasakannan, J. Peng, A new highly efficient method for the synthesis of rutile TiO_2. J. Alloys Compd. **585**, 75–77 (2014)
22. Y. Zou, X. Tan, T. Yu, Y. Li, Q. Shang, W. Wang, Synthesis and photocatalytic activity of chrysanthemum-like brookite TiO_2 nanostructures. Mater. Lett. **132**, 182–185 (2014)
23. K.H. Leona, P. Monash, S. Ibrahim, P. Saravanan, Solar photocatalytic activity of anatase TiO_2 nanocrystals synthesized by non-hydrolitic sol-gel method. Sol. Energy **101**, 321–332 (2014)
24. J.H. Lee, Y.S. Yang, Effect of hydrolysis conditions on morphology and phase content in the crystalline TiO_2 nanoparticles synthesized from aqueous $TiCl_4$ solution by precipitation. Mater. Chem. Phys. **93**, 237–242 (2005)
25. M. Chen, L. Hu, J. Xu, M. Liao, L. Wu, X. Fang, ZnO hollow-sphere nanofilm-based high-performance and low-cost photodetector. Small **17**, 2449–2453 (2011)